Geophys. J. R. astr. Soc. (1979) **57**, 609–638

Magnitude corrections for attenuation in the upper mantle

P. D. Marshall *Ministry of Defence, AWRE, Blacknest, Brimpton, Reading RG7 4RS*

D. L. Springer and H. C. Rodean *Lawrence Livermore Laboratory, University of California, Livermore, California 94550, USA*

Received 1978 October 30; in original form 1978 May 1

Summary. The $m_b : M_s$ relation for explosions at the Nevada Test Site (NTS) differs from those for explosions in other parts of the world. There is considerable evidence that this results mostly from high body-wave attenuation in the upper mantle beneath the western US. The authors have developed an empirical magnitude correction for body-wave attenuation and applied it to both source and receiver ends of the teleseismic body-wave path. The results imply that m_b values are lower for NTS explosions than for Soviet explosions of comparable yield and seismic coupling. The authors have also developed and applied a source-depth correction to account for pP–P interference in the P-wave arrival.

The body-wave magnitude resulting from these corrections is designated m_Q to distinguish it from other definitions of m_b. Values of m_Q determined for a world-wide set of large explosions show that a single m_Q: yield relation is a fair fit to the data for the explosions with high seismic coupling. However, grouping the explosions under two m_Q: yield relations gives a better fit to the data.

All the studied explosions in salt or granite or below the water table fit a common M_s: yield relation. Explosions from North America, Eurasia and Africa have a common $m_Q : M_s$ relation.

1 Introduction

The United States (US) and the Union of Soviet Socialist Republics (USSR) agreed in the Threshold Test Ban Treaty of 1974 July 3 that the yields of their underground nuclear weapons tests after 1976 March 31 will not exceed 150 kt. Each party to the treaty agreed to use national technical means for verifying compliance by the other party. In practice, this means that to estimate yields each party will use the observed seismic magnitudes of explosions at the other party's designated test sites.

Seismic monitoring for the Threshold Test Treaty includes detection, location and identification of seismic events, and (for events identified as explosions) yield estimation. One method for identifying exposions is the use of the $m_b : M_s$ discriminant, which is based on the observation that, for a given value of M_s, explosions generally have a m_b value one or two units greater than that of earthquakes.

In analysing $m_b : M_s$ discrimination plots, Liebermann & Pomeroy (1969) and Basham (1969) noted that the $m_b : M_s$ data for explosions and earthquakes in the western United States (WUS) are anomalous with respect to such data for the Aleutians, the Sahara and the USSR. Marshall & Basham (1972) confirmed that the $m_b : M_s$ relations for explosions in the WUS differ from those for explosions in the Aleutians, the USSR and China, but they did not detect any regional differences in $m_b : M_s$ data for earthquakes.

Evernden & Filson (1971) studied magnitude : yield relations for explosions in similar testing media at the Nevada Test Site (NTS) and at Amchitka in the Aleutian Islands. Their M_s : yield relation was the same for the two locations, but their m_b : yield relations were different.

These and other studies suggest that, for explosions in the WUS, either the M_s values are anomalously high, the m_b values are anomalously low or there is a combination of the two effects.

It has been proposed that tectonic strain release accompanying the explosions at NTS enhances M_s values, but Ward & Toksöz (1971), Toksöz & Kehrer (1972) and Massé (1973b) concluded that tectonic strain release alone does not have a sufficient effect on the M_s values for NTS explosions to account for the anomalous $m_b : M_s$ relation at NTS.

It has also been proposed that higher than average body-wave attenuation in the upper mantle beneath the WUS results in depressed m_b values for NTS explosions. Evernden & Filson (1971) cited evidence of significantly smaller P-wave amplitudes in the WUS compared with those in the eastern United States (EUS) and proposed that regional variations in body-wave attenuation are responsible for the different $m_b : M_s$ relation for explosions at NTS. Ward & Toksöz (1971), after rejecting M_s enhancement by tectonic strain release, concluded that regional variations in attenuation in the upper mantle are an important factor in regional variations of the $m_b : M_s$ relation. Marshall & Basham (1972) invoked upper-mantle attenuation to explain the differences in $m_b : M_s$ data between explosions in the WUS and explosions in the USSR in Kazakhstan and on Novaya Zemlya. Douglas *et al.* (1973) considered the effect of highly absorbing regions of the upper mantle on seismic-wave propagation and showed how large variations in P-wave amplitude (hence variation in m_b) can result from regional variations in upper-mantle properties.

In this paper, we assume that the $m_b : M_s$ relation for explosions at NTS is different from those for explosions in other regions because of relatively high body-wave attenuation in the upper mantle beneath the WUS. We examine the evidence for this assumption, develop a body-wave magnitude correction to account for regional variations in attenuation, and apply this correction to seismic data for a world-wide set of explosions.

2 Evidence for regional variations of attenuation in the upper mantle

Molnar & Oliver (1969) conducted a world-wide study of attenuation of the S_n waves in the upper mantle. They found that S_n propagation in the Basin and Range Province and the Colorado Plateau in the WUS is very inefficient compared to S_n propagation in the EUS. Solomon & Toksöz (1970) studied the attenuation of long-period teleseismic S and P waves and found high attenuation between the Rocky Mountains and the Sierra Nevada–Cascade ranges. Evernden & Clark (1970) showed that teleseismic P waves in the WUS are lower

in amplitude than those in the EUS by a factor of 3. They suggested that a region of abnormally low Q (the specific dissipation factor) exists beneath the WUS and that this low-Q region is probably related to the relatively high heat flow to the surface in the WUS. Solomon (1972) concluded that short-period ($T = 1$ s) body waves and long-period ($T > 20$ s) surface waves are attenuated more in the WUS than in the EUS, and that the 10- to 20-s surface waves used to determine M_s are attenuated at about the same rate throughout the United States. He also showed that Basham's (1969) $m_b : M_s$ data for 28 earthquakes in south-western North America show an apparent m_b depression of 0.3 to 0.4 magnitude units for earthquakes in the Basin and Range Province and under the Gulf of California with respect to earthquakes in adjacent areas. Booth, Marshall & Young (1974) determined amplitude corrections for long-period (16 s) and short-period (1 s) teleseismic P waves at 37 stations in the continental United States, Canada and the Aleutians. They found that short-period P waves are attenuated more in the WUS than in the EUS and attributed this attenuation pattern to lateral variations of Q in the upper mantle. Der, Massé & Gurski (1975) studied short-period teleseismic P and S waves at many stations throughout the continental United States and southern Canada. They found higher than average attenuation in the WUS, and noted that their geographic patterns of P- and S-wave attenuation generally agreed with observed patterns of P- and S-wave travel-time residuals, upper-mantle electrical conductivity and heat flow. Lee & Solomon (1975) used the measured attenuation of Love and Rayleigh waves in the western and east-central United States to infer the lithospheric thickness and the Q variation with depth in each of the two regions. They found that the value of Q^{-1} in the asthenosphere is about a factor of 2 greater beneath the WUS than beneath the east-central United States. Der & McElfresh (1976) determined average Q values for ray paths from the Salmon explosion in Mississippi to stations in the continental United States and eastern Canada. The Q values they determined for the WUS and eastern North America were consistent with the differences in m_b (0.3 to 0.4 magnitude units) observed between the WUS and EUS.

Regional variations in upper-mantle absorption are not confined to the United States. Berzon, Pasechnik & Polikarpov (1974) used P waves generated by surface axisymmetric sources at epicentral distances ranging from 1100 to 11 800 km and recorded at stations within the USSR (i.e. sources within and without the USSR) to investigate attenuation. They determined an average Q for various depth intervals in the mantle and crust beneath the USSR. Vinnik & Godzikovskaya (1972) found anomalously high P-wave attenuation, compared to the USSR average, in the mantle in two regions of the USSR: the Baikal Rift and the transitional zone between Asia and the Pacific Ocean. For the Baikal Rift, they showed correlations among Q, heat flow, geomagnetic sounding data and P_n velocity along a profile crossing the rift. Vinnik & Godzikovskaya (1975) extended this study to include central Asia and the central Asian part of the USSR in addition to eastern Siberia and adjacent ocean areas. They found anomalously high P-wave absorption in at least three types of tectonic structures: mid-ocean ridges, internal parts of the island arcs and regions of neotectonic platform activation.

We give, in Appendix A, the results of a study showing regional variations of P-wave absorption in the upper mantle. We considered, for test sites in the US and the USSR, the relationships between m_b and the P-wave period T used in determining m_b. The periods for signals from explosions at NTS are significantly lower than the periods observed from the Soviet sites. This difference in period is consistent with greater P-wave absorption in the WUS, but some of this difference could be caused by different seismic-coupling response of the rocks at these test sites.

In summary, anomalously high seismic-wave absorption in the upper mantle exists in at

least two tectonically similar regions within these continents: the Basin and Range Province in the WUS and the Baikal Rift in eastern Siberia in the USSR. These two regions differ markedly in other ways from stable shields and platforms in the continents: thin crust, high heat flow, and, in the upper mantle, high electrical conductivity, low density and low seismic velocities. It is beyond the scope of this paper to explore all the interrelations among these geophysical characteristics for regions of interest, but we do examine a few of them. In the long term, this might prove to be an important area of research for predicting the behaviour and propagation within and away from an inaccessible region in which a natural or man-made seismic disturbance occurs.

For our present purposes, we assume that there is a strong correlation between seismic absorption in the upper mantle and the P_n-wave velocity. In other words, our working hypotheses are that a relationship exists between P-wave velocity and Q in the upper mantle, and that P_n, the upper-mantle superficial velocity, is representative of the quality of the upper mantle. We have published a preliminary note on this correlation (Marshall & Springer 1976).

3 Method for correcting P-wave amplitudes

We have developed an empirical technique that corrects teleseismic P-wave amplitude for attenuation in the upper mantle. The correction is a function of the P_n-wave velocities (henceforth the P_n velocities) beneath the source (explosion) and the receiver (seismometer) locations. Our model is based, for the most part, on the analysis of data recorded in North America. We apply the technique to other regions of the world in a way that is consistent with the geophysical properties of those regions.

We have correlated magnitude residuals for specific recording stations with the measurements of P_n velocity beneath those stations. We have also obtained a relation between P_n velocity and $\bar{Q}_\alpha$, the effective Q_α for the upper mantle, in the following manner: we used published models of P-wave velocity and attenuation with depth in calculating the effective attenuation in the upper mantle and correlated these $\bar{Q}_\alpha$ values with the measured magnitude residuals. The details of the development of our method are described in the following sections.

3.1 STATION AMPLITUDE RESIDUALS AND P_n VELOCITY

Cleary (1967) and Booth *et al.* (1974) have published logarithmic amplitude residuals of teleseismic signals for Long Range Seismic Measurements (LRSM) stations of the North American network. Both sets of data exhibit the same trend of low amplitude in the WUS and high amplitudes in the EUS for short-period P waves. This trend has been noted by many other observers. It has also been noted that, where the P-wave amplitudes are low, the P_n velocities tend to be low and the P waves generally arrive late. Conversely, where the P-wave amplitudes are high, the P_n velocities tend to be high and the P waves usually arrive early. Our correlation between P_n velocities and P-wave travel-time residuals is given in Appendix B; our correlation between P_n velocities and P-wave amplitude residuals follows.

We have compared the P-wave $\log_{10}(A/T)$ residuals (Cleary 1967; Booth *et al.* 1974) with the P_n velocities beneath the recording stations (Herrin & Taggart 1962, 1968). The analysis technique used by Booth *et al.* was the same as that used by Cleary. In each analysis, the $\log_{10}(A/T)$ residual was determined by reference to the average $\log_{10}(A/T)$ residuals for discrete values of P_n velocity (in 0.5 km/s intervals). These results were previously published (Marshall & Springer 1976) and are presented in Table 1 and plotted in Fig. 1.

Table 1. $\text{Log}_{10}(A/T)$ residuals averaged for each incremental value of P_n velocity.

	$\text{Log}_{10}(A/T)$ residuals		
P_n velocity, km/s	Average	Standard deviation	Number of samples
7.75	−0.24	0.06	2
7.8	−0.15	0.09	14
7.85	−0.18	0.16	5
7.9	−0.16	0.10	4
7.95	−0.14	0.11	5
8.0	−0.8	0.16	5
8.05	−0.02	0.27	3
8.1	+0.15	0.10	11
8.15	−0.04[a]	0.04	5
8.2	+0.13	0.18	17
8.25	+0.18	0.13	3
8.3	+0.21	0.08	3

[a] Stations in Minnesota and Wisconsin.

Similar results have been published by North (1977). The curve through the data in Fig. 1 was drawn by hand and is an 'eyeball' fit to the data. A straight line through the data was considered but rejected for reasons involving absorption mechanisms, as discussed below.

3.2 RELATIONSHIP BETWEEN *P*-WAVE VELOCITY AND Q_α

Our next step was to relate the P_n velocity to a Q_α value for the crust and upper mantle. There are very few data relating these two quantities. Archambeau, Flinn & Lambert (1969), in their definitive paper on the fine structure of the upper mantle beneath North America, published a velocity-depth profile together with a Q_α-depth profile. These profiles were determined by matching arrival times and amplitudes from explosive sources in the WUS recorded at stations throughout the United States. Helmberger (1973) modelled *P*-wave seismograms for underground explosions in Nevada recorded within the WUS. In doing this, he assumed Q_α values in association with a velocity-depth profile. He used a Q_α value as low as 50 for the top of the low-velocity zone, and he used the Helmberger & Wiggins (1971) model HWNE for NTS to match the arrival times. The HWNE velocity-depth model is very similar to that of Archambeau *et al.* except that the velocity and Q_α at the top of the low-velocity zone are lower in the HWNE model.

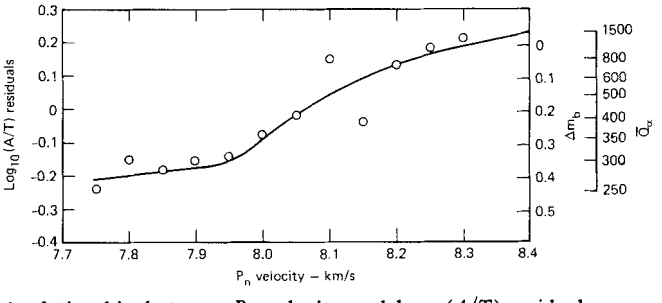

Figure 1. Observed relationship between P_n velocity and $\log_{10}(A/T)$ residuals, comparison with calculated Δm_b corrections and values of $\bar{Q}_\alpha$ for $T = 0.75$ s. The Δm_b and $\bar{Q}_\alpha$ are calculated from equation (3) for a travel time for 0 to 700 km of 80 s (see Table 4).

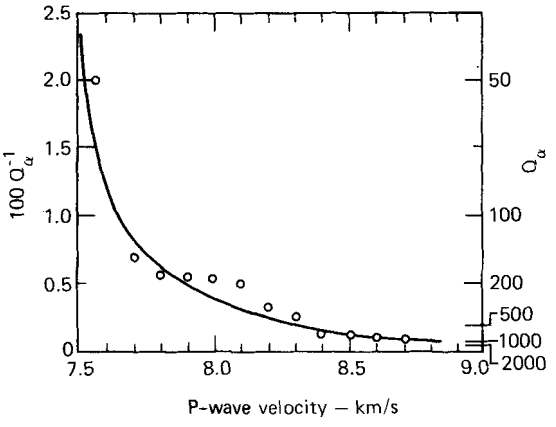

Figure 2. Relation between Q_α and *P*-wave velocity. The values of Q_α are taken from Archambeau *et al.* (1969) and Helmberger (1973).

In Fig. 2, we have plotted Q_α as a function of *P*-wave velocity; these data are taken directly from the results of Archambeau *et al.* and Helmberger. The curve drawn through these data is not intended as a best fit; it is used as an approximation to obtain $\bar{Q}_\alpha$ from velocity-depth profiles as described in the next section.

The data points in Fig. 2 are not from direct measurements of seismic-wave attenuation, but are inferred from comparisons of real and synthetic seismograms. A more definitive version of Fig. 2 could be developed from further theoretical and experimental investigations of the relation between *P*-wave velocity and Q_α in upper-mantle rocks at the appropriate temperatures and pressures.

One feature of the data points in Fig. 2 indicates that the curve relating *P*-wave velocity and Q_α is a valid approximation: the abrupt change in Q_α at a *P*-wave velocity of 8.1 km/s. Note that a similar change in δm_b is observed at the same velocity in Fig. 1. These characteristics in two independent sets of data suggest that the absorption mechanism or absorption properties are significantly different above and below 8.1 km/s. This supports the statement by Herrin & Taggart (1962) that 'variations in P_n velocity imply changes in the state or composition of the upper-most mantle'. The implication is that for high velocities the absorption is associated with processes at the grain boundaries, while for velocities less than 8 km/s the absorption is principally associated with partial melting or some other physical–chemical change in the upper-mantle rocks. Chung (1977) has suggested that changes in chemical composition in addition to partial melting are required to account for changes in P_n velocity from 8.1 to 7.8 km/s.

As part of our working hypothesis, we have made the key assumption that the Q_α:*P*-wave velocity relation shown in Fig. 2 is a valid relationship for rocks in the upper mantle. With this assumption, it is possible to calculate $\bar{Q}_\alpha$ values for the crust and upper mantle in regions of the world for which velocity-depth profiles are published.

3.3 CALCULATIONS OF $\bar{Q}_\alpha$ VALUES

The results of a sample calculation of $\bar{Q}_\alpha$ for the crust and upper mantle to a depth of 700 km are given in Table 2. We used the *P*-wave velocity versus depth profile CIT Model 111 (developed by Archambeau *et al.* 1969 for the Basin and Range Province) together with

Table 2. Example of $\bar{Q}_\alpha$ determination for CIT Model 111 of Basin and Range Province (Archambeau *et al.* 1969).

Increment depth (km)	Velocity (km/s)	Increment thickness (km)	Increment tt (s)	Cumulative $\int tt$ (s)	Q_α	Amplitude (A_i) at T = 0.5 s
0						1.0
14	6.0	14	2.33	2.33		
14.1	6.2	0.1	0.02	2.35	500	0.95
28	6.6	14	2.12	4.47		
28.1	6.7	0.1	0.01	4.48		
45	7.72	17	2.20	6.68		
60	7.719	15	1.94	8.62		
80	7.715	20	2.59	11.21	130	0.50
90	7.715	10	1.30	12.51		
120	7.719	30	3.89	16.40		
130	7.725	10	1.29	17.69		
140	7.74	10	1.29	18.98	140	0.47
146	7.8	6	0.77	19.75	170	0.46
148	7.9	2	0.25	20.00	210	0.46
170	8.325	22	2.64	22.64	590	0.45
180	8.335	10	1.20	23.84		
200	8.34	20	2.40	26.24	600	0.41
250	8.36	50	5.98	32.22		
300	8.435	50	5.93	38.15	710	0.39
350	8.53	50	5.86	44.01	800	0.37
375	8.63	25	2.90	46.91	1100	0.36
398	8.73	23	2.63	49.54	1200	0.36
400	9.10	2	0.22	49.76		
450	9.75	50	5.13	54.89		
500	9.80	50	5.1	59.99		
550	9.85	50	5.08	65.07		
600	9.90	50	5.05	70.12	2000	0.33
630	9.95	30	3.02	73.14		
645	10.00	15	1.50	74.64		
660	10.43	15	1.44	76.08		
680	10.93	20	1.83	77.91		
700	10.94	20	1.83	79.74		

Total travel time = 79.74 s. Resultant A = 0.33. $\bar{Q}_\alpha$ = 4.50.

the curve in Fig. 2 to obtain a profile of Q_α versus depth. We assumed that $Q_\alpha = 500$ in the crust. We then assumed a source with unit amplitude at the surface and used the relation

$$A_{i+1} = A_i \exp \frac{-\omega R}{2\alpha Q_\alpha} \tag{1}$$

to calculate in depth increments the attenuation of a downward-propagating P wave where: i = index of each increment, A = signal amplitude, ω = signal frequency, R = distance between depth for i and depth for $i + 1$, α = P-wave velocity.

We assumed a signal period of 0.5 s, but this arbitrary choice has no consequence if we also postulate that Q_α is independent of frequency in the bandwidth of interest. As shown in Table 2, we found $\bar{Q}_\alpha = 450$ for this model of the Basin and Range Province.

The results of this and similar calculations of $\bar{Q}_\alpha$ for various velocity-depth profiles to a depth of 700 km are given in Table 3(a). Table 3(b) gives some direct estimates of $\bar{Q}_\alpha$ for

three locations in the WUS, one location in the Pacific Ocean and the Soviet Union as a whole. Our calculations for the shield and platform regions of the world indicate $\bar{Q}_\alpha$ values of 800, the same value we obtained for the Herrin (1968) velocity-depth profile, which is a world-averaged model. On the other hand, our calculated $\bar{Q}_\alpha$ of 450 for the CIT 111 model of the Basin and Range Province by Archambeau *et al.* (1969) is significantly higher than our calculated value of 275 for the Helmberger & Wiggins (1971) HWNE model. The latter value is approximately the same as those derived from observations in the WUS (see Table 3(b)).

Let us assume that $\bar{Q}_\alpha = 800$ is representative for the crust and upper mantle of shield and stable platform areas – including the EUS, as indicated in Table 3(a) for Massé's (1973a) model. Let us also assume that $\bar{Q}_\alpha$ equals 275 for the Basin and Range Province, as indicated in Table 3(a) for the Helmberger & Wiggins (1971) model and in Table 3(b) for observations in the WUS. Then the corresponding difference in m_b values for common values of signal period can be calculated from the following relation, which is derived from equation (1):

$$\Delta m_b = m_{b_l} - m_{b_k} = (\bar{Q}_{\alpha_k}^{-1} - \bar{Q}_{\alpha_l}^{-1})(R/T\alpha)\pi \log_{10} e, \tag{2}$$

where: k = WUS, l = EUS, R/α = travel time to a depth of 700 km, T = period.

If $T = 0.75$ s (a representative value for the data sets of Cleary (1967) and Booth *et al.* (1974)), $\bar{Q}_{\alpha_k} = 275$, $\bar{Q}_{\alpha_l} = 800$ and $R/\alpha = 80$ s (a reasonable value, see Table 2), the result is

$$\Delta m_b = m_{b_l} - m_{b_k} = 0.35.$$

Table 3. Values of $\bar{Q}_\alpha$.

Area	Profile	$\bar{Q}_\alpha$	Reference
(a) Derived from velocity-depth profiles			
Nevada	HWNE	275	Helmberger & Wiggins (1971)
Shoal-Fallon NE	CIT112	575	Archambeau *et al.* (1969)
Shoal-Fallon SE	CIT111	450	Archambeau *et al.* (1969)
Colorado Plateau	Archambeau	600	Archambeau *et al.* (1969)
East-central US		790	Massé (1973a)
Western Russia		790	Massé & Alexander (1974)
Scandinavian Shield		790	Massé & Alexander (1974)
Canadian Shield		790	Massé & Alexander (1974)
World average	Herrin 68 travel time	800	Herrin (1968)
Australian Shield	SMAK I	790	Simpson, Mereu & King (1974)
Africa		670	Gumper & Pomeroy (1970)
Hindu Kush		1045	Kaila, Reddy & Narain (1968)
Central Asia, USSR		860	Lukk & Nersesov (1964)
Aleutian Islands	Down plate	1100	Sorrels, Crowley & Veith (1971)
	Through low velocity	330	Sorrels *et al.* (1971)
Shield	Standard LR	775	Ben-Menahem, Rosenman & Harkrider (1970)
Oceanic	Standard LR	410	Ben-Menahem *et al.* (1970)
Tectonic Continental	Standard LR	475	Ben-Menahem *et al.* (1970)
World with low-velocity zone	CIT208	580	Johnson (1969)
(b) Direct determinations			
NTS		210–260	Passechnik (1970)
NTS–WUS		260	Veith & Clawson (1972)
Tonto Forest Seismic Observatory (TSFO)		180–240	Kanamori (1967)
Tonga–Fiji (high absorption)		170	Barazangi & Isacks (1971)
USSR average		530 ± 150	Berzon *et al.* (1974)

This is within the observed differences of 0.3 to 0.4 magnitude units between the WUS and the EUS. This result is consistent with the relation in Fig. 1 giving $\log_{10}(A/T)$ residual versus P_n velocity for the P_n velocities of 7.8 to 7.9 km/s observed in the WUS and 8.2 to 8.3 km/s observed in the EUS. (The scales for Δm_b and $\bar{Q}_\alpha$ on the right side of Fig. 1 are based on the calculations for Table 4 that are described in the next section.)

Thus we believe that we have a credible two-part working hypothesis: a relationship exists between *P*-wave velocity and Q_α in upper-mantle rocks (Fig. 2), and P_n, the upper-mantle superficial velocity, indicates the quality of the upper mantle (Fig. 1) (Marshall & Springer 1976).

Furthermore, we believe that, given the P_n velocity, the absorption properties of the upper mantle can be estimated. Consequently, in magnitude determinations, amplitude corrections can be applied to source and receiver regions as appropriate.

3.4 FREQUENCY-DEPENDENT $\log_{10}A$ CORRECTIONS FOR ATTENUATION

We used the following variation of equation (2) to calculate the frequency-dependent $\log_{10}A$ corrections given in Table 4:

$$\log_{10}(A_n/A_m) = (T\bar{Q}_\alpha)_m^{-1} - (T\bar{Q}_\alpha)_n^{-1}(R/\alpha)\log_{10}\mathrm{e}, \tag{3}$$

where: m = reference condition, n = other conditions.

The corrections in Table 4 for the relative $\log_{10}$ amplitude as a function of frequency are referenced to $\bar{Q}_\alpha = 800$ and $T = 1$ s. The value of $\bar{Q}_\alpha = 800$ was selected as being representative of a stable shield or platform region where one can expect the least upper-mantle attenuation. The choice of $T = 1$ s is quite arbitrary and was chosen because it is the period most commonly associated with short-period, narrow-band recording systems.

In Table 4, the columns for $\bar{Q}_\alpha$, the $\log_{10}A$ corrections for $T = 0.75$ s, and the P_n velocity are consistent with the scales for Δm_b and $\bar{Q}_\alpha$ and with the curve relating $\log_{10}(A/T)$ residuals and P_n velocity in Fig. 1.

Table 4. $\mathrm{Log}_{10}A$ corrections as a function of $\bar{Q}_\alpha$ and T. The values are referenced to $\bar{Q}_\alpha = 800$, an average shield value, and $T = 1$ s, an average for short-period instruments.

	$\mathrm{Log}_{10}A$ correction as a function of the signal period T in seconds										
$\bar{Q}_\alpha$ for 0–700 km	0.50	0.75	0.80	0.85	0.90	1.00	1.10	1.20	1.25	1.50	P_n velocity, (km/s)
250	0.73	0.44	0.41	0.37	0.35	0.30	0.26	0.22	0.21	0.15	
260	0.69	0.40	0.38	0.35	0.33	0.27	0.24	0.21	0.19	0.14	7.75
275	0.65	0.39	0.36	0.33	0.30	0.26	0.22	0.19	0.18	0.13	7.80
280	0.62	0.37	0.34	0.31	0.28	0.24	0.21	0.17	0.16	0.12	7.90
300	0.59	0.35	0.31	0.29	0.26	0.22	0.19	0.16	0.15	0.11	7.95
350	0.48	0.28	0.25	0.23	0.21	0.17	0.14	0.12	0.11	0.07	8.00
400	0.40	0.22	0.20	0.18	0.16	0.13	0.11	0.09	0.08	0.05	
425	0.37	0.21	0.18	0.17	0.15	0.12	0.09	0.08	0.07	0.04	
450	0.35	0.18	0.16	0.15	0.13	0.10	0.08	0.06	0.06	0.03	
500	0.30	0.15	0.13	0.12	0.10	0.08	0.06	0.04	0.04	0.01	8.10
600	0.22	0.10	0.09	0.07	0.06	0.04	0.03	0.01	0.01	−0.02	8.15
700	0.17	0.07	0.05	0.04	0.03	0.02	0.00	−0.01	−0.01	−0.03	
750	0.15	0.06	0.04	0.03	0.02	0.01	−0.01	−0.02	−0.02	−0.04	8.20
800	0.13	0.04	0.03	0.02	0.01	0.00	−0.02	−0.03	−0.03	−0.05	
900	0.10	0.02	0.01	0.00	0.00	−0.02	−0.03	−0.04	−0.04	−0.05	8.25
1000	0.08	0.01	0.00	−0.01	−0.02	−0.03	−0.04	−0.05	−0.05	−0.06	8.30
1500	0.01	−0.04	−0.04	−0.05	−0.06	−0.07	−0.07	−0.08	−0.08	−0.09	8.40

The values of the $\log_{10}A$ corrections in Table 4 are positive for conditions with greater attenuation than the reference condition and are negative for conditions with less attenuation. This is consistent with the magnitude correction for attenuation that we describe in Section 4.

3.5 RECEIVER CORRECTION FOR ATTENUATION

The amplitude and duration of seismic signals recorded at a station are strongly influenced by the structure of the crust and upper mantle beneath that station. The signal characteristics are also affected by the coupling of the seismometer with the superficial layers of the crust. We recognized the importance of crustal response, but we did not have time to make estimates of this effect during the period available for the research reported here.

We have considered only the effect of attenuation in the upper mantle, and we have made estimates based on knowledge of the P_n velocity beneath each station. The P_n-velocity data are not available for all regions of the world, so we used data from only those seismic stations reporting to the International Seismological Centre (ISC) and the US Geological Survey for which P_n-velocity data near the stations have been reported. The sources of these

Table 5. Receiver corrections for attenuation. Reference numbers are given in the bibliography (Appendix E).

Station	P_n (km/s)	Δm_b	Ref.	Station	P_n (km/s)	Δm_b	Ref.	Station	P_n (km/s)	Δm_b	Ref.
AAM	8.3	0.01	16	HAL	8.11	0.14	12	RES	8.0	0.28	26
ALB	7.7	0.44	12	HFS	8.12	0.13	1	SCH	8.3	0.01	12
ALE	8.0	0.28	26	HYB	8.3	0.01	19	SCO	8.0	0.28	26
ALQ	7.8	0.39	16	INK	7.9	0.37	2	SCP	8.2	0.06	18
ASP	8.1	0.15	27	KEV	8.15	0.10	22	SES	8.08	0.18	12
ATL	8.2	0.06	6	KHC	8.2	0.06	10	SFA	8.15	0.10	2
ATU	7.9	0.37	11	KIR	7.84	0.38	1	SIBC	7.8	0.39	30
BLC	8.18	0.07	12	KJN	8.15	0.10	22	SKA	7.84	0.38	1
BMO	7.9	0.37	16	KON	8.05	0.21	25	SOD	8.15	0.10	22
CAR	8.1	0.15	9	KRK	8.15	0.10	22	STU	8.1	0.15	20
CLL	8.2	0.06	10	KTG	8.0	0.28	26	SUD	8.2	0.06	2
COL	8.1	0.15	14	LAO	8.1	0.15	16	SBQB	8.3	0.01	12
COP	8.1	0.15	17	LON	7.8	0.39	16	TFO	7.9	0.37	16
CPO	8.2	0.06	16	MBC	8.18	0.07	12	TRN	8.3	0.01	23
DAL	8.2	0.06	16	MNT	8.15	0.10	2	TRO	7.84	0.38	1
DUG	7.7	0.44	16	MOX	8.2	0.06	10	TUL	8.3	0.01	16
EDM	8.2	0.06	5	MUN	8.5	−0.06	8	UBO	7.90	0.37	16
EKA	8.1	0.15	21	NAO	8.05	0.21	25	UDD	7.84	0.38	1
ESK	8.1	0.15	21	NDI	8.3	0.01	19	UME	8.12	0.13	1
FBC	8.3	0.01	12	NOR	8.0	0.28	21	UPP	8.12	0.13	1
FCC	8.18	0.07	12	NPNT	8.18	0.07	12	VAL	8.1	0.15	3
FFC	8.3	0.01	15	NUR	8.15	0.10	22	VIC	7.8	0.39	12
FSJ	7.9	0.39	12	OTT	8.15	0.10	2	WEL	8.02	0.28	16
GBA	8.3	0.01	19	OXF	8.3	0.01	29	WES	8.1	0.15	16
GDH	8.0	0.28	26	PGBC	7.8	0.39	30	WRA	8.1	0.15	27
GEO	8.1	0.15	16	PHC	7.8	0.39	12	YKA	8.18	0.07	12
GIL	8.1	0.15	14	PMR	8.1	0.15	14	YKC	8.18	0.07	12
GOL	7.8	0.39	16	PNT	7.8	0.39	12				
GRF	8.2	0.06	10	POO	8.3	0.01	19				
GWC	8.18	0.07	12	PRU	8.2	0.06	10				

data are given in the bibliography. About 93 per cent of these data were obtained from P_n travel-time measurements; the remainder were estimated by other means.

The importance of receiver corrections for attenuation is clear. These corrections help remove one source of network amplitude bias and should produce more consistent magnitudes regardless of source location. For example, without receiver corrections an explosion recorded only at stations in the WUS would have a significantly lower magnitude than if it were recorded only in the EUS.

For this study, we estimated the amplitude correction for the receiver by noting the P_n velocity for each station, assuming a signal period of 0.75 s, and estimating the $\bar{Q}_\alpha$ from the relationship of Fig. 1. We did not attempt to be more precise because period data are not generally available in the ISC bulletins.

The stations used in this study and the station corrections estimated from P_n-velocity data are compiled in Table 5.

In general, the application of these receiver corrections increased the average value of the magnitudes (about 0.2 ± 0.1 m_b unit) but did not have much effect on the standard deviation of the mean magnitudes (± 0.2 m_b unit). The reason for the small effect on the standard deviations in this study is that most of the receivers for a given source region (e.g. NTS) tended to be in a fairly homogeneous tectonic area with respect to P_n velocity (e.g. the Canadian Shield). On the other hand, a study of the data used by Booth *et al.* (1974) from stations located in the WUS, EUS and Canadian Shield (7.8 km/s < P_n < 8.3 km/s) showed that the use of receiver corrections significantly reduced the variance of A/T due to station effects by a factor of 2 to 3. The statistics of receiver corrections is discussed further in Appendix C.

3.6 SOURCE CORRECTIONS FOR ATTENUATION AND DEPTH

We estimated amplitude corrections for attenuation in the source region in the same manner as for the receiver, except that we used a frequency-dependent correction as described in Section 4. Representative source-region corrections for attenuation, assuming $T = 0.75$ s, are presented in Table 6 for 10 locations or regions in which nuclear explosions have occurred: four in the US, one in Africa, one in India and four in the USSR. The source of the P_n-velocity data for these explosion locations are given in the bibliography (Appendix E).

We also developed an empirical source-depth correction in an attempt to account for the effect that the interference between the direct P wave and the surface reflection pP has on

Table 6. Source-region corrections for attenuation, assuming $T = 0.75$ s. Reference numbers are given in the bibliography (Appendix E).

Region	P_n (km/s)	Δm_b	Ref.
NTS, Nevada	7.8	0.39	16
Colorado	8.05	0.21	16
Amchitka	8.05	0.21	13
Mississippi	8.3	0.01	29
Sahara (Hoggar)	7.84	0.38	4
India	8.3	0.01	19
Caspian Basin	8.15	0.10	24
Bukhara	8.15	0.10	24
Kazakhstan	8.3	0.01	28
Pechora-Kama	8.4	−0.04	28

the teleseismic *P*-wave amplitude. This correction ranges in value from zero to approximately 0.2 m_b unit. The depth correction is discussed in detail in Appendix D.

4 Definition of a new magnitude, m_Q

In the preceding section we described a technique for determining *P*-wave amplitude corrections for upper-mantle attenuation at both the source and receiver ends of the signal path. In Appendix D, we describe a correction for the effect of interference from the surface reflection *pP*. We have formulated a new magnitude relation that includes these corrections. We call this new magnitude m_Q.

We used amplitude and period data from teleseismic recordings of explosion signals to calculate m_Q. Most of the amplitude and period data were taken from *Earthquake Data Report* (EDR) bulletins and, for some small explosions, from LRSM shot reports. P. Basham kindly supplied us with the basic Canadian data used in a publication on magnitude : yield relationships (Basham & Horner 1973). Supplementary amplitude data were taken from the ISC bulletins, which, regrettably, rarely include *P*-wave period data for the early explosions. Generally, only *P*-wave data recorded in the teleseismic range of 30° to 90° were used; however, it was necessary to use some data in the 20° to 30° range for the small explosions. As noted in the preceding section, we used data from only those stations for which an estimate of P_n velocity was available.

With these data, magnitude determinations at each individual station were made for a given explosion using the standard formulation:

$$m_1 = \log_{10}(A/T) + B(\Delta), \tag{4}$$

where A is displacement amplitude (in millimicrons) and T is period (in seconds) of the *P* wave. Individual station periods were also used to calculate an average period T_s (used later)

Table 7. Distance correction term $B(\Delta)$ from Booth *et al.* (1974).

Δ°	B(Δ)	Δ°	B(Δ)	Δ°	B(Δ)
30	3.77	50	3.70	70	3.75
31	3.77	51	3.71	71	3.76
32	3.77	52	3.72	72	3.77
33	3.77	53	3.73	73	3.78
34	3.76	54	3.74	74	3.79
35	3.75	55	3.75	75	3.79
36	3.73	56	3.76	76	3.78
37	3.71	57	3.77	77	3.77
38	3.70	58	3.78	78	3.76
39	3.69	59	3.79	79	3.75
30	3.68	60	3.79	80	3.75
41	3.68	61	3.78	81	3.76
42	3.67	62	3.80	82	3.78
43	3.67	63	3.80	83	3.80
44	3.66	64	3.78	84	3.81
45	3.67	65	3.77	85	3.82
46	3.68	66	3.75	86	3.84
47	3.68	67	3.73	87	3.86
48	3.69	68	3.72	88	3.87
49	3.70	69	3.73	89	3.88
				90	3.90

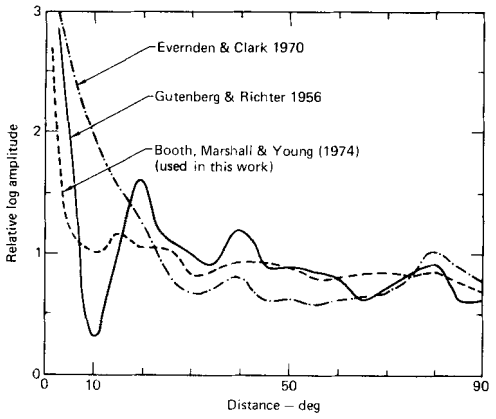

Figure 3. Representative distance-correction curves used in magnitude determination.

for a given explosion. The term $B(\Delta)$ is the distance-correction term derived by Booth *et al.* (1974). It is reproduced in Table 7 and is compared with other distance-correction curves in Fig. 3.

Our next step was to apply the receiver correction. Each receiver correction should, ideally, be adjusted for signal frequency. However, this was not possible so we applied a receiver correction from Table 4 based on an assumed signal period of 0.75 s. The resultant magnitude is

$$m_2 = m_1 + RC = \log_{10}(A/T) + B(\Delta) + RC, \tag{5}$$

where RC is the receiver correction that accounts for the estimated upper-mantle attenuation beneath the station. Next, we determined the average value of m_2 from the relation

$$\bar{m}_2 = \frac{1}{n} \sum_{i=1}^{n} m_{2,i}, \tag{6}$$

where n is the number of stations. Our definition of $\bar{m}_2$ is similar to the usual definition of m_b, but with a different kind of receiver correction. We then added the source correction for attenuation. This was obtained from Table 4 for the appropriate value of T_s and the estimate of P_n velocity for the source region. (Note that T data were not generally available from the ISC bulletins so the average period was determined from only EDR and LRSM data.) This magnitude formulation is

$$m_3 = \bar{m}_2 + SC(T) = \log_{10}(A/T) + B(\Delta) + RC + SC(T), \tag{7}$$

where $SC(T)$ is the source correction that accounts for the estimated upper-mantle attenuation.

Our final step was to correct for the interference of pP and P. The depth-correction ratio (equation (D1)) was calculated from known or estimated pP–P intervals and the observed T_s. The depth correction was determined from Fig. D2. The corresponding magnitude relation is

$$m_Q = m_3 + DC(T) = \log_{10}(A/T) + B(\Delta) + RC + SC(T) + DC(T), \tag{8}$$

where $DC(T)$ is the depth correction. This formula gives our final estimate of the magnitude of the explosion. *It is defined as m_Q to avoid any confusion with m_b.*

We give below an example of a typical calculation where m_2 and $\bar{m}_2$ are calculated for LRSM stations for which the P_n velocity and P-wave amplitude and period are known. The calculation uses the data given in Table 8.

The source-correction term, appropriate for $T_S = 0.93$ s and $P_n = 7.8$ km/s, is found from Table 4: $SC(T) = 0.28$. Therefore

$m_3 = 6.07 \pm 0.32$.

The explosion depth and an estimate of the average up-hole velocity give a pP–P interval time of 0.72 s. This interval time and the above value for T_S combine to give a depth-correction ratio (DCR) of 0.77. From Fig. D2, this gives a depth-correction term: $DC(T) = 0.10$. Therefore

$m_Q = 6.17 \pm 0.32$.

We have determined m_Q in this manner for all the explosions used in this study.

Table 8. Bilby explosion (data from LRSM shot report). Used for sample calculation of m_Q.

Station	$\text{Log}_{10}(A/T)$	T (s)	Δ (deg)	$B(\Delta)$	$RC(T)$	m_2
BLVW	1.91	1.0	27.5	3.75	0.06	5.72
BRPA	2.04	1.2	29.1	3.77	0.04	5.85
ORFL	2.42	1.0	30.4	3.77	0.06	6.25
DHNY	1.55	0.8	31.9	3.77	0.15	5.47
HNME	1.98	0.9	36.6	3.72	0.15	5.85
NPNT	2.40	0.8	39.4	3.69	0.07	6.16
OONW	1.70	0.8	73.2	3.78	0.21	5.69
SBGR	1.48	0.9	81.9	3.78	0.06	5.32

$T_S = 0.93 \pm 0.14$ s[a] $\quad \bar{m}_2 = 5.70 \pm 0.32$[a]

[a] Errors are the standard deviations for the sample.

5 Applications of m_Q

5.1 m_Q AND M_S VERSUS YIELD

We have determined m_Q values for a world-wide set of 46 nuclear explosions and two large chemical explosions for which yield data are available. We have also determined M_S values for 43 of the 46 nuclear explosions using the procedure developed by Marshall & Basham (1972). The results are tabulated in Table 9 and are plotted in Figs 4–8.

Of these 48 explosions, 38 were detonated by the US, seven by the USSR (including the two chemical explosions), two by France and one by India. The yields, depths of burial and other data for the 38 American explosions were published by Springer & Kinnaman (1971, 1975, in preparation). The Soviets have announced and described the two chemical explosions, which were used to form a rock-slide dam near Alma-Ata (Aptikayev *et al.* 1967). They have also described, but not specifically located or dated, a number of peaceful nuclear explosions (PNEs) some of which have been identified by others with specific seismic events (Nordyke 1975). The Kazakh I event of 1965 January 15 near Semipalatinsk is identified with the '1004' cratering explosion, and the Pechora-Kama event of 1971 March 23 is believed to be the row-charge cratering experiment near the southern end of a proposed canal converting the Pechora and Kama rivers. The two Bukhara events of

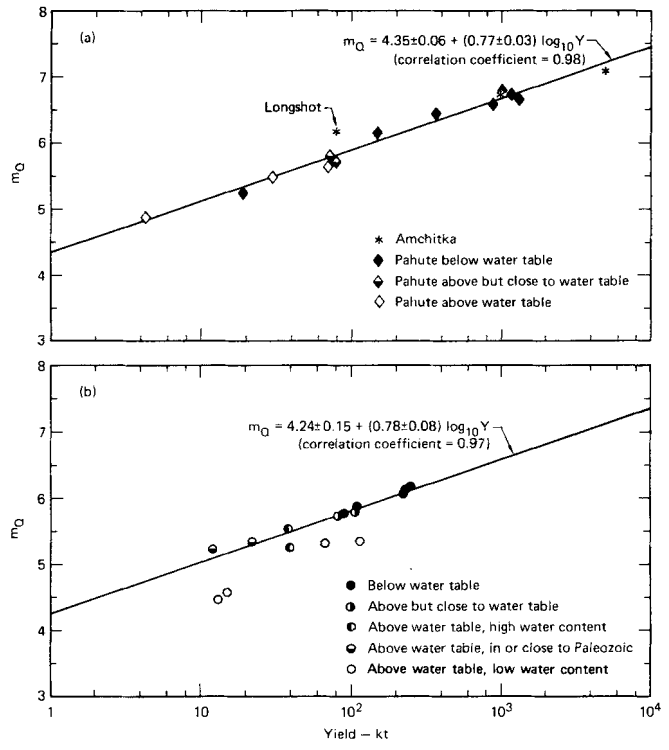

Figure 4. Plots of m_Q versus yield for explosions: (a) on Amchitka Island and at Pahute Mesa, NTS, and (b) at Yucca Flat, NTS. The calculation for the line in (b) does not include Mississippi, Haymaker, Delphinium and Fisher (shots above the water table and in strata with low water content).

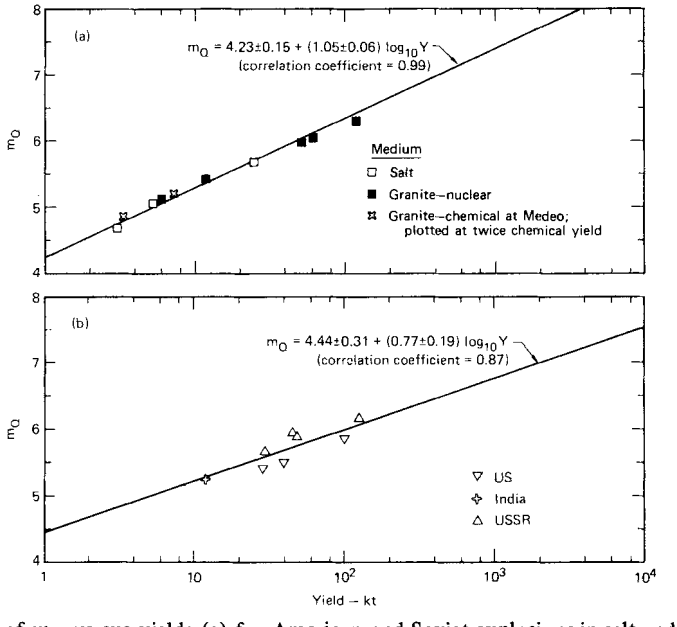

Figure 5. Plots of m_Q versus yield: (a) for American and Soviet explosions in salt and American, French and Soviet explosions in granite, (b) for PNEs in the US, India and the USSR. The Medeo shots were not included in calculating the line in (a).

Table 9. Magnitude for explosions with known yields.[a]

Location or medium	Explosion	$n(m_Q)$	$\bar{m}_2$	$\bar{T}_S$ (s)	SC	m_3	$pP-P$ (s)	DC	m_Q	$\pm SD$	M_S	$n(M_S)$	Y (kt)
(a) Amchitka Island and Pahute Mesa, NTS													
Amchitka	Cannikin	34	6.89	1.22	0.08	6.97	1.00	0.12	7.09	0.35	6.69	45	<5000
	Milrow	38	6.52	1.01	0.12	6.64	0.74	0.08	6.72	0.44	5.05	21	~1000
	Longshot	32	6.03	0.89	0.15	6.18	0.45	0.00	6.18	0.41	3.96	18	~80
Pahute Mesa	Handley	28	6.48	1.23	0.18	6.66	0.95	0.10	6.76	0.31	5.36	5	>1000
	Boxcar	25	6.36	1.19	0.19	6.55	0.96	0.12	6.67	0.29	5.21	61	1300
	Benham	30	6.39	1.20	0.19	6.58	1.10	0.17	6.75	0.28	5.29	7	1150
	Greeley	22	6.23	1.17	0.21	6.44	0.97	0.13	6.57	0.27	5.09	23	870
	Half Beak	21	6.08	1.00	0.26	6.34	0.72	0.08	6.42	0.33	4.68	16	365
	Scotch	22	5.69	0.96	0.28	5.97	0.91	0.19	6.16	0.25	4.39	11	155
	Knickerbocker	13	5.36	0.88	0.31	5.67	0.56	0.04	5.71	0.22	3.96	10	76
	Chartreuse	13	5.39	0.86	0.31	5.70	0.59	0.07	5.77	0.24	3.56	18	73
	Duryea	7	5.31	0.92	0.29	5.60	0.59	0.04	5.64	0.23	3.30	15	70
	Schooner	3	4.95	0.80	0.36	5.31	0.12	0.16	5.47	0.10	3.39	4	30
	Rex	7	4.89	0.88	0.31	5.20	0.60	0.06	5.26	0.28	3.47	9	19
	Palanquin	2	4.26	0.70	0.43	4.69	0.09	0.20	4.89	0.18	2.54	6	4.3
(b) Yucca Flat, NTS; high-coupling explosions and low-coupling explosions													
Below water table	Commodore	24	5.89	1.16	0.21	6.10	0.84	0.08	6.18	0.27	4.39	9	250
	Bilby	8	5.79	0.93	0.28	6.07	0.72	0.10	6.17	0.32	4.40	29	235
	Carpetbag	20	5.87	1.20	0.19	6.06	0.67	0.01	6.07	0.28	4.33	9	220
	Calabash	14	5.69	1.22	0.19	5.88	0.70	0.01	5.89	0.24	4.06	13	110
	Starwort	15	5.57	1.10	0.22	5.79	0.57	0.00	5.79	0.26	3.81	6	90
Above but close to water table	Flask	22	5.59	1.13	0.21	5.80	0.54	0.00	5.80	0.28	3.71	11	105
	Miniata	14	5.50	1.03	0.26	5.76	0.54	0.00	5.76	0.28	3.74	6	83
High water content above water table	Aardvark	3	5.00	0.97	0.27	5.27	0.49	0.00	5.27	0.18	3.37	9	40
	Par	4	4.97	0.70	0.43	5.40	0.58	0.13	5.53	0.26	2.43	15	38
In or very near Palaeozoic sedimentary rocks above water table	Discus Thrower	7	4.98	0.83	0.33	5.31	0.41	0.01	5.32	0.20	2.85	3	22
	Handcar	4	4.88	0.83	0.33	5.21	0.37	0.00	5.21	0.21	2.80	17	12

In dry porous media above water table	Mississippi	6	4.99	0.95	0.28	5.27	0.60	0.04	5.31	0.26	3.30	23	115
	Haymaker	5	4.85	0.76	0.39	5.24	0.56	0.08	5.32	0.21	3.09	6	67
	Delphinium	3	4.23	0.80	0.36	4.59	0.40	0.00	4.59	0.48	–	–	15
	Fisher	1	4.00	0.75	0.39	4.39	0.52	0.07	4.46	–	2.56	4	13
(c) American and Soviet explosions in salt; American, French and Soviet explosions in granite													
Salt	US Gnome	2	4.13	0.60	0.52	4.65	0.36	0.03	4.68	0.11	–	–	3.1
	US Salmon	11	4.87	0.66	0.03	4.90	0.58	0.16	5.06	0.27	2.85	18	5.3
	USSR Caspian	17	5.59	0.80	0.09	5.68	0.43	0.00	5.68	0.36	3.67	6	25
Granite	US Hardhat	5	4.66	0.82	0.36	5.02	0.17	0.08	5.10	0.21	2.90	33	5.9
	US Shoal	4	5.01	0.76	0.39	5.40	0.21	0.03	5.43	0.10	3.27	26	12
	US Piledriver	27	5.71	0.95	0.28	5.99	0.24	0.05	6.04	0.26	3.82	20	62
	FR Ruby	8	5.62	0.99	0.25	5.87	Est.	0.10	5.97	0.31	–	–	52
	FR Saphir	14	5.88	0.88	0.29	6.17	Est.	0.12	6.29	0.30	4.10	8	120
	USSR Medeo I	–	4.61	0.70	0.06	4.67	Shallow	0.20	4.87	0.10	–	–	1.69[b]
	USSR Medeo II	–	4.95	0.70	0.06	5.01	Shallow	0.20	5.21	0.18	–	–	3.60[b]
(d) Peaceful nuclear explosions in the US, India and the USSR													
	US Rio Blanco	11	5.31	0.83	0.33	5.64	1.30	0.20	5.84	0.24	3.97	23	3 × 33 = 100
	US Rulison	18	4.94	0.84	0.33	5.27	1.57	0.20	5.47	0.27	3.60	59	40
	US Gasbuggy	11	5.07	0.75	0.13	5.20	0.87	0.20	5.40	0.42	3.37	22	29
	India	8	5.03	0.74	0.01	5.04	0.01	0.20	5.24	0.24	3.20	3	12
	USSR Kazakh I	13	5.95	0.74	0.01	5.96	Shallow	0.20	6.16	0.39	3.90	1	125
	USSR Pechora-Kama	21	5.66	0.83	0.5	5.71	Shallow	0.20	5.91	0.25	4.28	15	3 × 15 = 45
	USSR Bukhara I Clay	8	5.36	0.83	0.08	5.44	Deep	0.20	5.64	0.31	3.79	4	30
	USSR Bukhara II Salt	15	5.59	0.86	0.08	5.67	Deep	0.20	5.87	0.33	3.89	8	47

[a] *Notes:*

n Number of stations used to determine m_Q and M_S. $\bar{m}_2$ Defined in equation (6); similar to standard body-wave magnitude m_b. $\bar{T}_S$ Mean period of signal. *SC* Source correction from Table 4. m_3 Defined in equation (7). *pP–P* Surface reflection delay time. *DC* Depth correction from Fig. 3. m_Q Defined in equation (8). ± *SD* Standard deviation of m_Q. M_S Surface-wave magnitude. *Y* Explosion yield.

[b] Chemical explosions. Nuclear equivalent ≈ chemical yield × 2 (i.e. Medeo I = 3.38 kt, Medeo II = 7.20 kt).

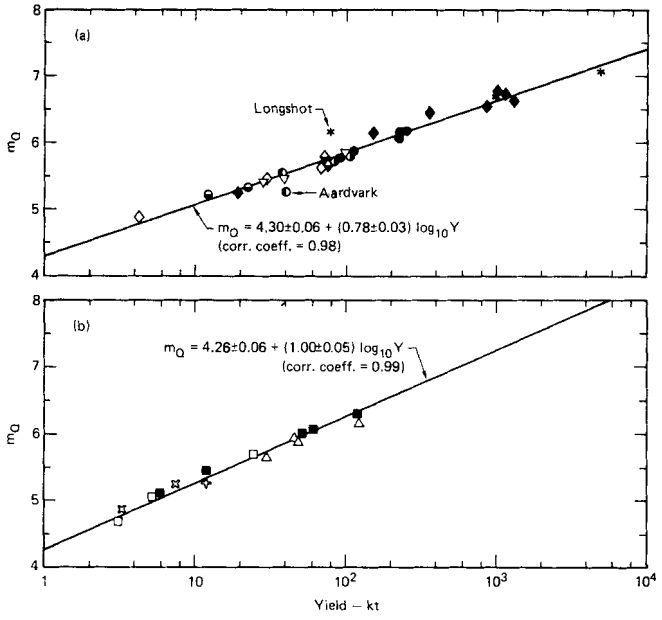

Figure 6. Plots of m_Q versus yield for selected explosions: (a) at Amchitka, Pahute Mesa and Yucca Flat (excluding Mississippi, Haymaker, Delphinium and Fisher) and PNEs in the WUS, (b) in salt and granite and PNEs in India and the USSR. Two of the USSR PNEs were for cratering and two for extinguishing gas-well fires. The Medeo shots were not included in calculating the line in (b). See Figs 4 and 5 for definitions of symbols.

1966 September 30 and 1968 May 21 are believed to be the explosions used to seal two gas wells with runaway fires. We *assume* that the 25-kt explosion in salt described by the Soviets is the event of 1968 July 1 north of the Caspian Sea. The French have detonated a total of 13 explosions in a granitic massif of the Hoggar in the Sahara (Duclaux & Michaud 1970); the yields of the explosions on 1963 October 18 and 1965 February 27 have been published (SIPRI 1968; Ferrieux & Guereini 1971; Marshall, Douglas & Hudson 1971). The Indian explosion on 1974 May 18 has been described (Chidambaram & Ramanna 1975).

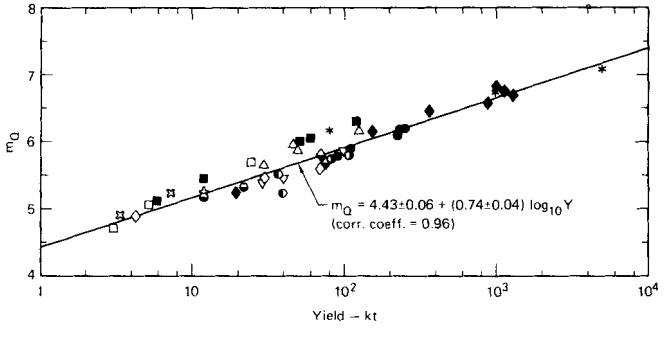

Figure 7. Plot of m_Q versus yield for all explosions except low-coupling explosions at Yucca Flat (Mississippi, Haymaker, Delphinium and Fisher). The Medeo shots were not included in calculating the line. See Figs 4 and 5 for definitions of symbols.

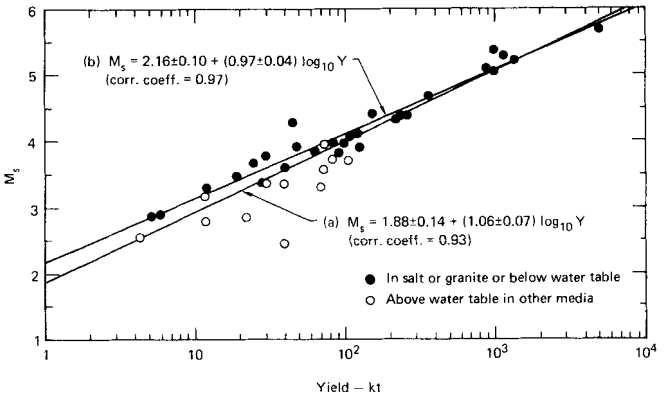

Figure 8. Plot of M_S versus yield for all nuclear explosions except low-coupling explosions at Yucca Flat (Mississippi, Haymaker, Delphinium, Fisher), Gnome and Ruby. Line (a) gives the result of the linear regression analysis for all the explosions shown. Line (b) gives the result for the explosions in salt or granite or below the water table.

As shown in Fig. 4(a), the m_Q: yield relation for Amchatka has a distinctly different slope than that for Pahute Mesa. The Pahute Mesa m_Q: yield relation has relatively little scatter and appears to be independent of the location of the explosion with respect to the water table. If it were not for Longshot, the Amchitka and Pahute Mesa explosions would appear to have a common m_Q: yield relation.

The Yucca Flat data in Fig. 4(b) show more scatter than the Pahute Mesa data, but the scatter is considerably reduced if four of the explosions above the water table (Mississippi, Haymaker, Delphinium and Fisher) are ignored. For this reason, these four explosions are not considered further in this body-wave magnitude : yield discussion. The other explosions above the water table appear to have had seismic coupling similar to that of explosions below the water table: Flask and Miniata were close to the water table, Aardvark and Par were in media with high water content and Discus Thrower and Handcar were very near or in the Palaeozoic sedimentary rocks.

As shown in Fig. 5(a) all the explosions in salt and granite, including the chemical explosions (plotted at twice the chemical yield*) appear to have a common m_Q: yield relation.

In Fig. 5(b), the US PNEs appear to have had lower coupling than the explosions in India and the USSR.

After considering the m_Q: yield relations implied in Figs 4 and 5, we decided that the data tend to fall into the two groups presented in Fig. 6. In Fig. 6(a), the m_Q for Longshot is relatively high and that for Aardvark is relatively low; otherwise the explosions appear to have a common m_Q: yield relation. All the data in Fig. 6(b) appear to have a common m_Q: yield relation. The appearance of Fig. 7, in which all explosion data are plotted, confirms the existence of two m_Q: yield relations, although a single relation is a fair approximation.

The available M_s data for all explosions listed in Table 9, except the four low-coupling explosions at Yucca Flat, are plotted in Fig. 8. The scatter is considerably greater than that in Fig. 7, but is reduced if *all explosions above the water table* (except those in salt or granite) are dropped from the data set. Then the only explosion with an anomalous value

* A standard rule of thumb relating the seismic-signal generating efficiency of chemical and nuclear explosions.

of M_S is the Pechora-Kama cratering explosion; data for the others closely follow a common M_S : yield relation.

5.2 m_Q VERSUS M_S

As noted in Section 1, it was discovered some years ago that $m_b : M_S$ relations for explosions at NTS differ from $m_b : M_S$ relations for explosions in other parts of the world. We determined M_S in addition to m_Q values for 43 of the 48 explosions listed in Table 9. Twenty-eight of these 43 explosions were at NTS. The m_Q versus M_S data for all 43 explosions are plotted in Fig. 9 along with results of the linear regression of the data.

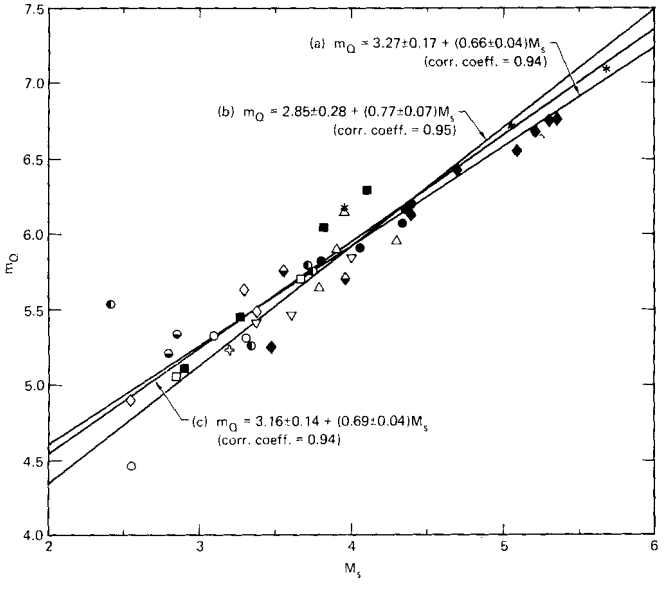

Figure 9. Plot of m_Q versus M_S for all nuclear explosions (for which M_S data are available) that are listed in Table 9. Line (a) is for NTS explosions and Shoal, line (b) for other explosions, and line (c) for all explosions. See Figs 4 and 5 for definitions of symbols.

The above results show that it is reasonable to fit a common $m_Q : M_S$ relation to the data for all 43 explosions, including the four low-coupling explosions above the water table in Yucca Flat. Only Par and perhaps Fisher appear anomalous. The above data have one deficiency: 32 of the 43 explosions were in the WUS; only 11 of the 43 were in other parts of the world.

The deficiency does not exist in the $m_b : M_S$ data set for explosions in the US and the USSR developed by Marshall & Basham (1972). They considered 28 explosions in the US, 26 of which were at NTS and 28 explosions in the USSR, 22 of which were at the principal test sites in Kazakhstan (20) and on Novaya Zemlya (2). Location and magnitude data for these explosions are presented in Tables 10 and 11. The $m_b : M_S$ relations for these explosions are compared to their $m_Q : M_S$ relations in Figs 10 and 11. Clearly the $m_b : M_S$ data for NTS are anomalous with respect to the data for explosions in other areas, while the $m_Q : M_S$ data for NTS are much less so. This is substantiated by the linear-regression relations presented in the figures.

Table 10. M_s, m_b, and m_Q data for US explosions.

Explosion	M_s	m_b	m_Q
Halfbeak	4.71	6.04	6.46
Dumont	4.08	5.51	5.93
Piledriver	3.76	5.56	5.98
Tan	3.85	5.55	5.97
Greely	5.04	6.05	6.47
Scotch	4.35	5.51	5.93
Piranha	3.87	5.37	5.79
Chartreuse	3.64	5.15	5.57
Bronze	3.64	5.26	5.68
Pinstripe	2.74	4.46	4.88
Buff	3.55	5.17	5.59
Corduroy	3.90	5.43	5.85
Charcoal	3.31	4.91	5.33
Discus Thrower	2.94	4.73	5.15
Cup	3.54	4.94	5.36
Faultless	5.07	6.26	6.68
Boxcar	5.45	6.29	6.71
Lanpher	3.88	5.66	6.08
Zaza	4.12	5.70	6.12
Yard	3.28	4.93	5.35
Commodore	4.42	5.77	6.19
Gasbuggy	3.46	4.81	5.43
Knickerbocker	3.96	5.14	5.56
Wagtail	3.58	5.32	5.74
Diluted Waters	2.53	4.55	4.97
Lampblack	3.25	4.91	5.33
Longshot	3.96	6.06	6.17
Milrow	5.00	6.60	6.71

Data taken from Basham (1969) and M_s recalculated using method of Marshall & Basham (1972).

6 Conclusions

There is considerable evidence that relatively high body-wave attenuation in the upper mantle beneath the NTS is a principal cause of the different m_b:M_s relation for NTS explosions. Our empirical correction for attenuation implies that m_b values for NTS explosions are about 0.3 magnitude unit less than the values for explosives with comparable yields and seismic coupling at the Soviet test sites. A single m_Q:yield relation is a fair fit to the data for the explosions with high seismic coupling. However, grouping the explosions under two m_Q:yield relations gives a better fit to the data.

Our M_s values for the explosions showed that all explosions either in salt or granite or below the water table fit a common M_s:yield relation. This suggests that explosions are less efficient in generating surface waves if there is little or no competent or water-saturated rock above the explosion.

As a consequence of our results in Figs 6, 7, 9 and 11, we believe that the relations shown in Fig. 1 between magnitude residuals and P_n velocity and in Fig. 2 between Q_α and P velocity are good first approximations to reality. We believe that the use of m_Q is preferable to the use of m_b in estimating the yields of explosions throughout the world.

More research in seismology, upper-mantle geochemistry and geophysics, and the

Table 11. M_S, m_b and m_Q data for USSR explosions.

Explosion No.[a]	Area	M_S	m_b	m_Q
1	Kazakh	3.45	5.16	5.33
2	Kazakh	2.95	4.90	5.10
3	Kazakh	3.30	5.28	5.45
4	Kazakh	3.59	5.48	5.64
6	Kazakh	3.56	5.39	5.55
8	Kazakh	3.72	5.55	5.70
9	Kazakh	3.63	5.86	6.01
12	Kazakh	3.14	5.18	5.35
13	Kazakh	3.56	5.59	5.74
14	Kazakh	3.48	5.22	5.39
15	Kazakh	3.16	5.30	5.47
16	Kazakh	3.39	5.25	5.42
17	Kazakh	3.50	5.44	5.60
23	Kazakh	3.50	5.24	5.41
25	Kazakh	4.10	5.99	6.17
27	Kazakh	3.68	5.68	5.83
29	Kazakh	3.68	5.58	5.73
30	Kazakh	3.53	5.16	5.33
33	Kazakh	3.53	5.41	5.57
34	Kazakh	3.36	5.32	5.49
5	N. Caspian	3.68	5.66	5.81
18	Urals	3.57	4.85	5.37
19	Urals	3.32	4.77	5.29
22	Caspian	3.42	5.64	5.80
26	E. Caspian	3.97	5.89	6.04
31	Urals	3.50	4.82	5.22
11	Novaya Zemlya	4.43	6.16	6.56
24	Novaya Zemlya	4.41	6.16	6.56

[a] Explosion numbers refer to epicentral list of Basham & Marshall (1972).

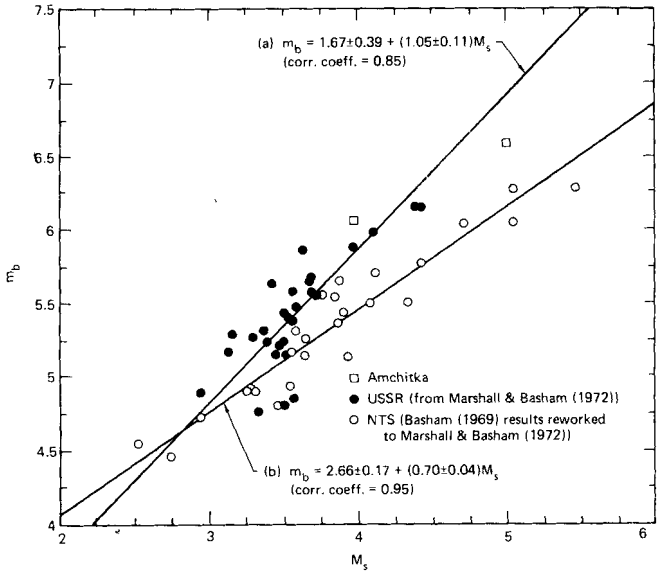

Figure 10. Plot of m_b versus M_S for nuclear explosions in North America and the USSR. Values of M_S were calculated from results of Marshall & Basham (1972). Line (a) is for Amchitka and Soviet explosions, line (b) for NTS explosions.

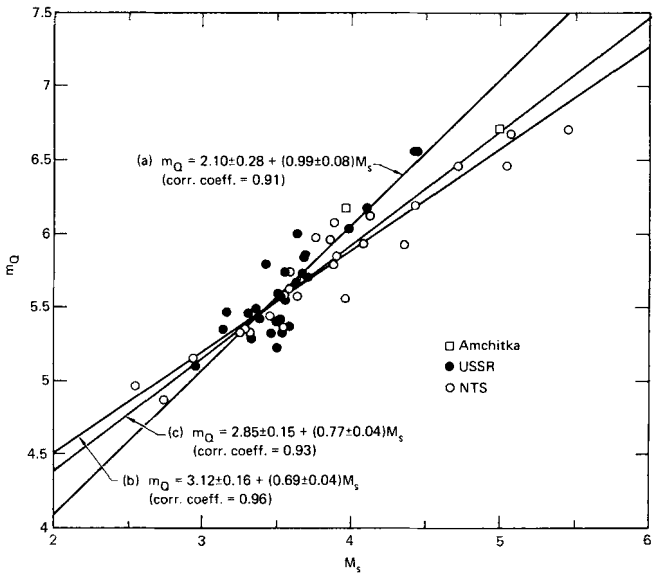

Figure 11. Plot of m_Q versus M_S for nuclear explosions in North America and the USSR. Line (a) is for Amchitka and Soviet explosions, line (b) for NTS explosions and line (c) for all the explosions shown.

theoretical and experimental aspects of seismic-wave absorption in rocks is needed before definitive, proven corrections of the kind we have proposed will be available.

Acknowledgments

Work performed under the auspices of the US Department of Energy by the Lawrence Livermore Laboratory under contract number W-7405-Eng-48. Work supported in part by the UK Ministry of Defence and the US Defense Advanced Research Projects Agency.

References

Aptikayev, F. F., Gurbunova, I. V., Dokutyaev, M. M., Melovatskii, B. V., Nersesov, I. L., Rautian, T. G., Romaskov, A. N., Rulev, B. G., Fornitiev, A. G., Chalturin, V. I. & Charin, D. A., 1967. The results of scientific observations during the Medeo explosion, *An. Kaz. S.S.R. Vestnik*, **5**, 30–40 (in Russian).

Archambeau, D. B., Flinn, E. A. & Lambert, D. G., 1969. Fine structure of the upper mantle, *J. geophys. Res.*, **74**, 5825–5865.

Barazangi, M. & Isacks, B., 1971. Lateral variation of seismic wave attenuation, *J. geophys. Res.*, **76**, 8493–8516.

Basham, P. W., 1969. Canadian magnitudes of earthquakes and nuclear explosions in south-western North America, *Geophys. J. R. astr. Soc.*, **17**, 1–13.

Basham, P. W. & Horner, R. B., 1973. Seismic magnitudes of underground nuclear explosions, *Bull. seism. Soc. Am.*, **63**, 105–132.

Basham, P. W. & Marshall, P. D., 1972. *Seism. Series Earth Phys. Branch No. 63*, Department of Energy, Mines and Resources, Earth Physics Branch, Ottawa, Canada.

Ben-Menahem, A., Rosenman, M. & Harkrider, D. G., 1970. Fast evaluation of source parameters from isolated surface wave signals. Part I, Universal tables, *Bull. seism. Soc. Am.*, **60**, 1337–1387.

Berzon, I. S., Pasechnik, I. P. & Polikarpov, A. M., 1974. The determination of *P*-wave attenuation values in the Earth's mantle, *Geophys. J. R. astr. Soc.*, **39**, 603–611.

Booth, D. C., Marshall, P. D. & Young, J. B., 1974. Long and short period *P*-wave amplitudes from earthquakes in the range 0–114°, *Geophys. J. R. astr. Soc.*, **39**, 523–537.

Chidambaram, R. & Ramanna, R., 1975. Some studies on India's peaceful nuclear explosion experiment (IAEA-TC-1-4/19), in *Peaceful Nuclear Explosions IV*, pp. 421–436, International Atomic Energy Agency, Vienna.

Chung, D. H., 1977. P_n velocity and partial melting – Discussion, *Tectonophys.*, **42**, T35–T42.

Cleary, J., 1967. Analysis of the amplitudes of short-period *P* waves recorded by Long Range Seismic Measurements stations in the distance range 30° to 102°, *J. geophys. Res.*, **72**, 4705–4712.

Der, Z. A., Massé, R. P. & Gurski, J. P., 1975. Regional attenuation of short-period *P* and *S* waves in the United States, *Geophys. J. R. astr. Soc.*, **40**, 85–106.

Der, Z. A. & McElfresh, T. W., 1976. Short-period *P*-wave attenuation along various paths in North America as determined from *P*-wave spectra of the Salmon nuclear explosion, *Bull. seism. Soc. Am.*, **66**, 1609–1622.

Douglas, A., Marshall, P. D., Gibbs, P. G., Young, J. B. & Blamey, C., 1973. *P* signal complexity re-examined, *Geophys. J. R. astr. Soc.*, **33**, 195–221.

Duclaux, F. & Michaud, L., 1970. Conditions experimentales des tirs nucleaires souterrains français au Sahara, 1961–1966, *C. R. Acad. Sci. Paris*, **270B**, 189–192.

Evernden, J. F. & Clark, D. M., 1970. Study of teleseismic P.II–Amplitude data, *Phys. Earth planet. Int.*, **4**, 24–31.

Evernden, J. F. & Filson, J., 1971. Regional dependence of surface-wave versus body-wave magnitudes, *J. geophys. Res.*, **76**, 3303–3308.

Ferrieux, H. & Guereini, C., 1971. Effects mechaniques d'une explosion nucleaire contenue (IAEA-PL-429/19), in *Peaceful Nuclear Explosions II*, pp. 253–273, International Atomic Energy Agency, Vienna.

Gumper, F. & Pomeroy, P. W., 1970. Seismic wave velocities and earth structure on the African continent, *Bull. seism. Soc. Am.*, **60**, 651–668.

Helmberger, D. V., 1973. On the structure of the low velocity zone, *Geophys. J. R. astr. Soc.*, **34**, 251–263.

Helmberger, D. V. & Wiggins, R., 1971. Upper mantle structure of midwestern United States, *J. geophys. Res.*, **76**, 3229–3245.

Herrin, E., 1968. 1968 seismological tables for *P* phases, *Bull. seism. Soc. Am.*, **58**, 1223–1225.

Herrin, E., 1969. Regional variations of *P*-wave velocity in the upper mantle beneath North America, in *The Earth's Crust and Upper Mantle*, pp. 242–246, Monograph No. 13, American Geophysical Union, Washington, DC.

Herrin, E. & Taggart, J., 1962. Regional variations in P_n velocity and their effect on the location of epicenters, *Bull. seism. Soc. Am.*, **52**, 1037–1046.

Herrin, E. & Taggart, J, 1968. Source bias in epicenter determinations, *Bull. seism. Soc. Am.*, **58**, 1791–1796.

Horai, K. & Simmons, G., 1969. Spherical harmonic analysis terrestrial heat flow, *Earth planet. Sci. Lett.*, **6**, 386–394.

Johnson, L. R., 1969. Array measurements of *P* velocities in the lower mantle, *Bull. seism. Soc. Am.*, **59**, 973–1008.

Kaila, K. L., Reddy, P. R. & Narain, H., 1968. *P*-wave travel times from shallow earthquakes recorded in India and inferred upper mantle structure, *Bull. seism. Soc. Am.*, **58**, 1879–1897.

Kanamori, H., 1967. Spectrum of short-period core phases in relation to the attenuation in the mantle, *J. geophys. Res.*, **72**, 2181–2186.

Lee, W. B. & Solomon, S. C., 1975. Inversion schemes for surface wave attenuation and Q in the crust and mantle, *Geophys. J. R. astr. Soc.*, **43**, 47–71.

Liebermann, R. C. & Pomeroy, P. W., 1969. Relative excitation of surface waves by earthquakes and underground explosions, *J. geophys. Res.*, **74**, 1575–1590.

Lilwall, R. C. & Douglas, A., 1970. Estimation of *P*-wave travel times using the joint epicentre method, *Geophys. J. R. astr. Soc.*, **19**, 165–181.

Lukk, A. A. & Nersesov, I. L., 1964. Structure of the upper mantle as shown by observations of earthquakes of intermediate focal depth, *Dokl. Akad. Nauk SSR*, **162**, 559–562 (in Russian).

Marshall, P. D. & Basham, P. W., 1972. Discrimination between earthquakes and underground explosions employing an improved M_S scale, *Geophys. J. R. astr. Soc.*, **28**, 431–458.

Marshall, P. D., Douglas, A. & Hudson, J. A., 1971. Surface waves from underground explosions, *Nature*, **234**, 8–9.

Marshall, P. D. & Springer, D. L., 1976. Is the velocity of P_n an indicator of Q_α? *Nature*, **264**, 531–533.

Massé, R. P., 1973a. Compressional velocity distribution beneath central and eastern North America, *Bull. seism. Soc. Am.*, **63**, 911–935.

Massé, R. P., 1973b. Radiation of Rayleigh wave energy from nuclear explosions and collapse in southern Nevada, *Geophys. J. R. astr. Soc.*, **32**, 155–185.

Massé, R. P. & Alexander, S. S., 1974. Compressional velocity distribution beneath Scandinavia and western Russia, *Geophys. J. R. astr. Soc.*, **39**, 587–602.

Molnar, P. & Oliver, J., 1969. Lateral variations of attenuation in the upper mantle and discontinuities in the lithosphere, *J. geophys. Res.*, **74**, 2648–2682.

Nordyke, M. D., 1975. A review of Soviet data on the peaceful uses of nuclear explosions, *Annals of Nuclear Energy*, **2**, 657–673, Pergamon Press, New York.

North, R. G., 1977. Station magnitude bias – its determination, causes, and effects, *Massachusetts Institute of Technology Lincoln Laboratory Technical Note 1977–24*, Lexington, Massachusetts.

Pasechnik, I. P., 1970. *Characteristics of Seismic Waves from Nuclear Explosions and Earthquakes*, Nauka Publishing House, Moscow (in Russian). *Geo. Bull.*, Series A, Nos 7–12, ARPA Order No. 189–1, The Rand Corporation, Santa Monica, California (English translation).

Simpson, D. W., Mereu, R. F. & King, D. W., 1974. An array study of *P*-wave velocities in the upper mantle transition zone beneath northwestern Australia, *Bull. seism. Soc. Am.*, **64**, 1757–1788.

SIPRI, 1968. *Seismic Methods for Monitoring Underground Explosions*, rapporteur D. Davies, Stockholm International Peace Research Institute, Stockholm.

Solomon, S. C., 1972. On *Q* and seismic discrimination, *Geophys. J. R. astr. Soc.*, **31**, 163–177.

Solomon, S. C. & Toksöz, M. N., 1970. Lateral variation of attenuation of *P* and *S* waves beneath the United States, *Bull. seism. Soc. Am.*, **60**, 819–838.

Sorrels, G. G., Crowley, J. B. & Veith, K. F., 1971. Methods for computing ray paths in complex geological structures, *Bull. seism. Soc. Am.*, **61**, 27–53.

Springer, D. L., 1974. Secondary sources of seismic waves from underground nuclear explosions, *Bull. seism. Soc. Am.*, **64**, 581–594.

Springer, D. L. & Kinnaman, R. L., 1971. Seismic source summary for U.S. underground nuclear explosions, 1961–1970, *Bull. seism. Soc. Am.*, **61**, 1073–1098.

Springer, D. L. & Kinnaman, R. L., 1975. Seismic source summary for U.S. underground nuclear explosions, 1971–1973, *Bull. seism. Soc. Am.*, **65**, 343–349.

Toksöz, M. N. & Kehrer, H. H., 1972. Tectonic strain release by underground nuclear explosions and its effect on seismic discrimination, *Geophys. J. R. astr. Soc.*, **31**, 141–452.

Veith, K. F. & Clawson, G. E., 1972. Magnitude from short period *P*-wave data, *Bull. seism. Soc. Am.*, **62**, 435–452.

Vinnik, L. P. & Godzikovskaya, A. A., 1972. Sounding of the Earth's mantle by the method of seismically conjugate points, *Bull. (Izv.) Acad. Sci. USSR, Earth Phys.*, **10**, 656–664 (English edition).

Vinnik, L. P. & Godzikovskaya, A. A., 1975. Lateral variations of the absorption by the upper mantle beneath Asia, *Bull. (Izv.) Acad. Sci. USSR*, **1**, 3–15 (English edition).

Ward, R. W. & Toksöz, M. N., 1971. Causes of regional variation of magnitudes, *Bull. seism. Soc. Am.*, **61**, 649–670.

Appendix A: *P*-wave periods and teleseismic magnitudes

We briefly investigated the relation between teleseismic magnitudes and *P*-wave periods for explosions at three test sites: NTS in the US and the two principal Soviet test sites in Kazakhstan and on Novaya Zemlya. Our data source was the EDR bulletins published by the US Geological Survey/National Earthquake Information Service. The results for 49 explosions at NTS, 38 presumed explosions in Kazakhstan and eight on Novaya Zemlya are presented in Fig. A1. The NTS explosions were in Yucca Flat, Rainier Mesa, Pahute Mesa and the Climax Stock.

There is little difference between the results for the two Soviet sites, so a common $T_s : m_b$ relation is shown for these sites. However, there is a distinct difference between the results for NTS and those for Soviet sites. For a given value of m_b between 4.5 and 7, the *P*-wave period is 0.3 to 0.4 s greater for NTS explosions than for presumed Soviet explosions. This is consistent with Table 6, which, according to our hypothesis that P_n

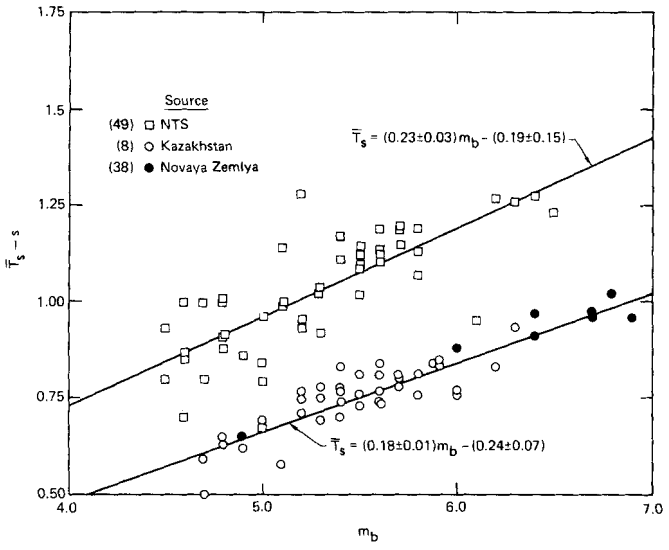

Figure A1. *P*-wave periods ($\bar{T}_s$) and teleseismic magnitudes (m_b) for explosions. Data source: *Earthquake Data Report* (USGS/NEIS). The error indicated in the equations is one standard deviation.

velocity is related to Q_α, indicates greater attenuation beneath NTS than beneath the Kazakhstan site. (The P_n-velocity data were not available for Novaya Zemlya.)

However, the longer periods for signals from NTS could be caused, at least in part, by differences in seismic coupling between the newer rocks at NTS and the much older rocks at the two sites in the USSR. Therefore, we cannot regard the evidence in Fig. A1 as definitive proof that there is greater attenuation in the upper mantle beneath NTS than beneath the sites in Kazakhstan and on Novaya Zemlya. Clearly this is a topic worthy of further research.

Appendix B: P_n velocities and *P*-wave travel-time residuals

As stated in Sections 2 and 3, our working hypotheses are that a relationship exists between *P*-wave velocity and Q in the upper mantle, and that P_n, the upper-mantle superficial velocity, represents the quality of the upper mantle. It follows from the relationships between $\bar{Q}_\alpha$ and P_n velocity in Fig. 1 and Q_α velocity in Fig. 2 that low values of P_n velocity imply low *P*-wave velocities, possibly a low-velocity zone, in the upper mantle. Therefore, a station in a region of low P_n velocity should record longer teleseismic travel times than a station in a region of high P_n velocity. This trend is suggested by the results of studies of *P*-wave seismic delay times and P_n velocity in North America (e.g. Herrin & Taggart 1968; Herrin 1969).

We investigated teleseismic travel-time data for as many stations as possible with known or estimated P_n velocities. We used the travel-time station residuals published by Lillwall & Douglas (1970). We attempted to correct their data for station elevation above sea level by assuming an upper-crustal velocity of 4 km/s and normalizing the data to sea level. The regression analysis for height-corrected data (shown in Fig. B1) is

$$\delta t_p = -5.93\,P_n + 47.46. \qquad \text{(B1)}$$

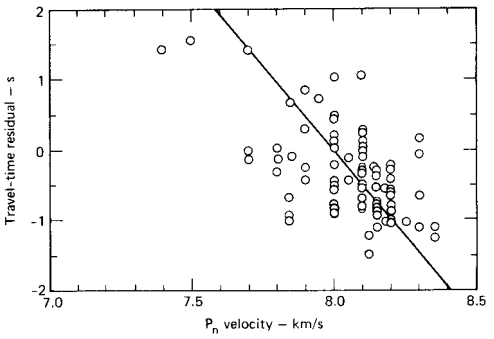

Figure B1. Relation between P_n velocity and P-wave travel-time residuals. Data source: Lilwall & Douglas (1970). Corrected for station elevation assuming a crustal velocity of 4 km/s.

The height correction shifts the station residuals a bit but does not alter the trend for longer travel times (positive residuals) with lower P_n velocities. This result has the same trend as that obtained by Horai & Simmons (1969):

$$\delta t_p = -2.22\, P_n + 17.62. \tag{B2}$$

These results are consistent with our working hypotheses.

Appendix C: statistics of the receiver correction

The intent of our receiver correction, which is described in Section 3, is to remove what may be described as 'receiver network bias'. As shown in Tables 4 and 5, the effect of receiver network corrections is generally to increase the average magnitude ($\bar{m}_2 > \bar{m}_1$), but the reverse effect ($\bar{m}_1 > \bar{m}_2$) is possible in the case of sufficiently high P_n velocities and signal periods at most or all of the stations. Our receiver corrections will reduce the standard deviation or variance of the magnitude only in certain circumstances. For example, if all the stations are located in an area with a uniform value of P_n velocity, the receiver corrections will affect the mean magnitude but not the standard deviation. On the other hand, if the stations are located in areas with wide variations of P_n velocity, the receiver corrections will affect both the mean and the standard deviation of the magnitude.

In Section 3, we noted that the receiver corrections in this study increased the average value of the magnitudes (about 0.2 ± 0.1 m_b unit) but did not have much effect on the standard deviations of the magnitudes (± 0.02 m_b unit). The principal reason for this small effect on the standard deviations is that most of the receivers for a given source region (e.g. NTS) tended to be in the fairly homogeneous tectonic area with respect to P_n velocity (e.g. the Canadian Shield).

The example discussed in Section 4 and presented in Table 8 used data from only eight stations. The receiver corrections for five of the stations were relatively small (0.04 to 0.07); those for the other three were relatively large (0.15 to 0.21). As noted by one referee, $\bar{m}_1 = 5.69 \pm 0.34$ and $\bar{m}_2 = 5.70 \pm 0.32$; a change which seems barely significant.

The large quantity of LRSM data analysed by Booth *et al.* (1974) provides a better demonstration of the effect of our receiver correction on the mean magnitude and its standard deviation. These data were recorded at widely separated stations located in the WUS, EUS and Canadian Shield. P_n velocity for these station locations ranges from 7.8 to 8.3 km/s, approximately. The data were recorded on standardized equipment and were

Table C1. Effect of receiver corrections for data of Booth *et al.* (1974).

Item	Case 1	Case 2	Case 3
Mean A/T	1.619	1.825	1.761
Total degrees of freedom	1591	1591	1591
Number of samples	2696	2696	2696
Sum of squares attributable to station effects	54.530	20.096	22.742
Number of stations	36	36	36
Variance attributable to stations	1.515	0.558	0.632

measured according to a systematic procedure. As in Booth *et al.* (1974), we estimated the contributions of a source term, a distance term and a station term to A/T. In addition, we considered three cases as shown in Table C1:

Case 1. A and T data with no receiver correction.
Case 1. A and T data with receiver corrections assuming $T = 0.75$ s (as in this study).
Case 3. A and T data with receiver corrections for the observed T.

The application of any significance tests to the contents of Table C1 will show that the receiver corrections are highly significant and that our use of receiver corrections is justified. Note that assuming $T = 0.75$ s in the receiver corrections increased the mean A/T value somewhat more than using the observed period. Also note that, in both Cases 2 and 3, the receiver corrections for P_n velocity reduced the variance of A/T due to station effects by a factor of 2 to 3.

Appendix D: source-depth corrections

The amplitude of the P wave within the first few cycles of the seismogram is measured for use in magnitude determination. The initial cycles of an explosion seismogram consist of the direct P wave plus the contribution from the free-surface reflection, pP. Thus explosions of the same yield fired at different depths will generate a teleseismic P-wave amplitude that is a function of depth as illustrated in Fig. D1.

To obtain consistent magnitude : yield relationships, we must correct for this variation in P-wave amplitude with explosion depth. The arrival time of pP and, therefore, the effect on P-wave amplitude can often be estimated. The frequency content of the signal must also be considered in correcting for source depth. Consider an explosion that generates a P-wave with a period $T = 1$ s followed 0.5 s later by a phase-reversed pP signal with the same period. The direct P and the reflected pP waves will interfere constructively as illustrated in Fig. D1(b). On the other hand, if the explosion is at the same depth but of much lower yield so that the dominant frequency is higher (say $T = 0.5$ s), then the pP reflection will follow the

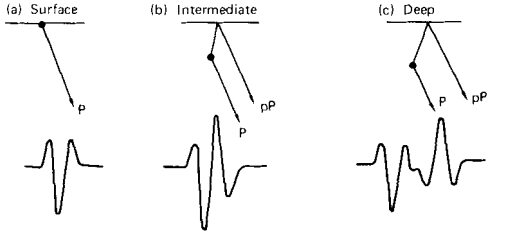

Figure D1. Variation of the pP–P interference effect with explosion depth.

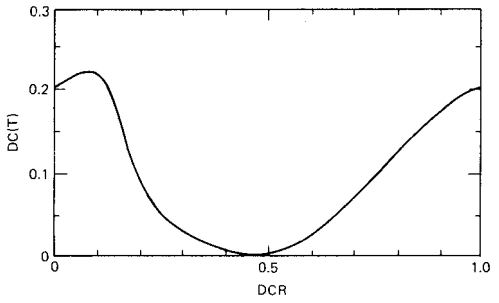

Figure D2. The magnitude-correction term $DC(T)$ given as a function of the depth-correction ratio DCR. The $DC(T)$ is added to magnitude m_3 equation (8) to give the final magnitude m_Q.

direct P with the same delay of 0.5 s – too late for interference with the direct P – resulting in a signal like that in Fig. D1(c).

To account for these effects, we have introduced a depth correction ratio (DCR), which is defined as:

$$DCR = \frac{pP\text{–}P \text{ interval (in seconds)}}{P\text{-wave period (in seconds)}}. \tag{D1}$$

We have developed an empirical curve of P-wave amplitude as a function of DCR for use in estimating the variation of P-wave amplitude caused by pP interference. This correction is illustrated in Fig. D2. The correction is in terms of the logarithm of the amplitude, the form used in the magnitude formulae in Section 4. The logarithmic correction has a maximum value of about 0.2, which corresponds to almost a factor of 2 in yield for magnitude : log-yield relations with a slope of 0.8 to 0.9.

The pP–P time can be estimated from either data for depth of burial and up-hole velocity (preferable) or depth-determination techniques like cepstral methods or spike filtering. The estimated pP–P time is divided by the average period of the observed teleseismic P wave to obtain the DCR. The log-amplitude correction corresponding to the appropriate DCR is determined from Fig. D2 and *added* to the averaged magnitude m_3 as described in Section 4. By adding the correction, all explosions are normalized to the maximum amplitude corresponding to the case of constructive interference. By subtracting the correction, explosions would be normalized to the amplitude of the single, direct P wave from the explosion. We arbitrarily chose the former case of *adding* the depth correction.

The correction shown in Fig. D2 was derived, assuming elastic reflection, from a series of theoretical solutions for superimposed P and pP waves with different delay times. This is an oversimplified model because of the complications added by geological layering, surface spall, etc. For example, it appears that pP may be small when the signal from spall closure is large and vice versa (Springer 1974). Multipathing can also complicate matters by constructive or destructive interference with direct P (Douglas *et al.* 1973). Such multipathing can not only affect the amplitudes of the first arrivals but also can cause erroneous depth solutions from cepstral or spike-filtering techniques.

Appendix E: bibliography

SOURCES OF P_n VELOCITY DATA FOR RECEIVER AND SOURCE LOCATIONS

1 Båth, M., 1971. Average crustal structure of Sweden, *Pure Appl. Geophys.*, **88**, 75–91.
2 Berry, M. J., 1973. Structure of the crust and upper mantle in Canada, *Tectonophys.*, **20**, 183–201.

3 Bott, M. H. P. & Watts, A. B., 1971. Deep structure of the continental margin adjacent to the British Isles. ICSU/SCOR Working Party 31 Symposium, Cambridge 1970, *Inst. Geol. Sci. Rep. No. 70/14*, pp. 89–109.

4 Choudbury, M. A. & Rothé, J. P., 1965. Durée de propagation des ondes *P*; anomalie vers 20°, *Extr. Ann. Geophys.*, **21**, 266–272 (in French).

5 Cumming, G. L. & Kaneswich, E. R., 1966. Crustal structure in Western Canada, *Final Report, Contract AF 19 (628)-2835 AFCRL*, Bedford, Massachusetts.

6 Dorman, L. M., 1966. Studies of the seismicity of the State of Georgia, Phases I and II, *Semi-annual technical report No. 4*, Georgia Institute of Technology, Atlanta.

7 Eiby, G. A., 1957. The Wellington Profile and the Pencarrow Profile, N.Z.D.S.I.R., *Geophys. Div. geophys. Mem. No. 5.*

8 Everingham, I. B., 1965. The crustal structure of the southwest of western Australia. Bureau of Mineral Resources, Geology and Geophysics, Department of National Development, *Report No. 1965/97*, Commonwealth of Australia.

9 Fiedler, G. B., 1966. Private communication.

10 Fuchs, K. & Landisman, M., 1966. Detailed crustal investigation along a north–south section through the central part of western Germany, *The Earth beneath the Continents*, AGU Physical Monograph, **10**, 433–452.

11 Galanopoulos, A. G., 1966. Private communication.

12 Goodacre, A. K., 1972. Generalized structure and composition of the deep crust and upper mantle in Canada, *J. geophys. Res.*, 77, 3146–3161.

13 Guidroz, R. R., Linville, F., Harley, T. W., Bauer, R. E., McDermott, J. G., Howard, R. F., McNeely, G. D. & Median, A. R., 1968. Preliminary analysis report – Aleutian Islands experiment – ocean Bottom experiments, *ARPA Order No. 624*, Texas Instruments, Inc., Dallas, Texas.

14 Hales, A. L. & Asada, T., 1966. Crustal structure in coastal Alaska, *The Earth beneath the Continents*, AGU Physical Monograph, **10**, 420–432.

15 Hall, D. H. & Hajnal, Z., 1973. Deep seismic crustal studies in Manitoba, *Bull. seism. Soc. Am.*, **63**, 885–910.

16 Herrin, E. & Taggart, J., 1962. Regional variations in P_n velocity and their effect on the location of epicentres, *Bull. seism. Soc. Am.*, **52**, 1037–1046.

17 Hirschleber, H., Hjelme, J. & Sellevol, M. A., 1966. A refraction profile through northern Jutland. Working group on the Skaggerak project, Paper No. 1, *Geodetisk Institute Meddelelse No. 41.*

18 Howell, B. F., 1961. Geophysical studies of the Appalachian area, *Miner. Indust.*, **30**, 1–8, February.

19 Kaila, K. L., Reddy, P. R. & Narain, H., 1968. *P* wave travel times from shallow earthquakes recorded in India and inferred upper mantle structure, *Bull. seism. Soc. Am.*, **58**, 1879–1897.

20 * Knopoff, L., Mueller, S. & Pilant, W. L., 1966. Structure of the crust and upper mantle in the Alps from phase velocity of Rayleigh waves, *Bull. seism. Soc. Am.*, **56**, 1009–1044.

21 Parks, R., 1967. Seismic refraction networks, *PhD thesis*, University of Edinburgh, Scotland.

22 Pentilla, E., 1969. Structure of the Earth's crust in Finland as revealed by data on the propagation velocities of seismic waves, *Bull. (Ivz.) Acad. Sci. USSR, Earth Phys.*, **5**, 280–283 (English edition).

23 Robson, G. R., 1966. Private communication.

24 Ryaboy, V. Z. & Shchuykin, Yu, K., 1975. Upper mantle inhomogeneities and seismicity, *Bull. (Izv.) Acad. Sci. USSR, Earth Phys.*, 7, 419–424 (English edition).

25 Sellevol, M. A. & Warwick, R. E., 1971. A refraction study of the crustal structure in southern Norway, *Bull. seism. Soc. Am.*, **61**, 457–471.

26 * Tryggvason, E., 1964. Arrival times of *P* waves and upper mantle structure, *Bull. seism. Soc. Am.*, **54**, 727–736.

27 Underwood, R., 1967. The seismic network and its applications, *PhD thesis*, Australian National University, Canberra, Australia.

28 Volvoskii, I. C., 1973. *Seismic Investigation of the Earth's Crust in the USSR*, Nedra Publishing House, Moscow (in Russian).

29 Warren, D. H., Healy, J. H. & Jackson, W. H., 1966. Crustal seismic measurements in southern Mississippi, *J. geophys. Res.*, 71, 3437–3458.

30 White, W. R. H. & Savage, J. C., 1965. A seismic refraction and gravity study of the Earth's crust in British Columbia, *Bull. seism. Soc. Am.*, **55**, 463–486.

* Indicates results were not determined from refraction profiles.